

Robustness of planar random graphs to targeted attacks

J.-P. Kownacki*

*Laboratoire de Physique Théorique et Modélisation,
CNRS-Université de Cergy-Pontoise - UMR 8089 ,
2 avenue Adolphe Chauvin, 95302 Cergy-Pontoise Cedex, France*

In this paper, robustness of planar trivalent random graphs to targeted attacks of highest connected nodes is investigated using numerical simulations. It is shown that these graphs are relatively robust. The nonrandom node removal process of targeted attacks is also investigated as a special case of non-uniform site percolation. Critical exponents are calculated by measuring various properties of the distribution of percolation clusters. They are found to be roughly compatible with critical exponents of uniform percolation on these graphs.

Keywords: Percolation problems (Theory); Random graphs, networks; Critical exponents and amplitudes (Theory).

I. INTRODUCTION

Robustness or fragility of a graph characterize its behavior when systematic or random deletion of a fraction of nodes is performed. These questions are of practical importance for real complex networks (World Wide Web, social networks, cells, etc) and, recently, there has been much interest in investigating targeted and random attacks for two families of random complex networks [1, 2, 3], namely exponential and scale-free networks [4]. Resilience to random deletion of nodes can, for example, be seen as tolerance against error, *i.e.* random failure of a fraction of nodes. Targeted deletion of high degree nodes can simulate attacks of hackers on computer networks. However, besides these practical issues, investigating random and targeted attacks on abstract graphs is of great theoretical interest in its own right. It has to be noted that the random attack problem is equivalent to uniform site percolation [5].

In this paper, we study a family of purely abstract random graphs extensively used in the past decades as discrete models for euclidean quantum gravity [6], namely random Φ^3 planar graphs. These planar graphs are made of trivalent vertices and look locally like the regular honeycomb lattice. But the faces are not necessarily hexagonal, so that long distance properties are very different from those of honeycomb lattices. Note that site percolation on these graphs has already been investigated [7, 8]. By means of Monte-Carlo simulations, we study resilience of these graphs against targeted attacks defined as a systematic face removal process, *i.e.* removal of all links and vertices that belong to the edges of the targeted face. More precisely, we investigate connected clusters distributions when all faces whose number of edges is larger than a cut-off k_{max} are removed.

A key feature in the behavior of graphs against targeted attacks is the degree distribution. However, vertex coordination numbers on complex networks are uncorrelated random variables so that the degree distribution is sufficient to characterize these random graphs. On the contrary, planarity constraints induce long range correlations for random Φ^3 planar graphs so that the degree distribution is not enough to characterize these graphs [9]. This characteristic is also shared by Voronoï/Delaunay graphs. However, correlations in the latter case decrease much faster than for random Φ^3 planar graphs. This fundamental difference between complex networks and random Φ^3 planar graphs induces radically different behaviors under uniform percolations problems. The main purpose of this work is then to determine whether it also induces different behaviors against non-uniform percolation like targeted attacks, and, if so, to quantify these differences.

It has to be noted that, even if random Φ^3 planar graphs have been used in Euclidean quantum gravity, the problem studied here is not relevant to these issues. Indeed, there is no back-reaction of any degree of freedom on the connectivity of the graphs. In other words, the disorder due to random degree distribution is quenched and we study the average behavior against targeted attacks of a graph picked at random in the ensemble of random Φ^3 planar graphs. However, this work could be the starting point of the study of a modified model of quantum gravity characterized by matter fields (Ising spin, for instance) coupled to the ensemble of graphs obtained from the random Φ^3 planar graphs after a systematic node deletion procedure.

Besides the size of the largest connected component S , we study several properties of connected cluster of graphs for various values of k_{max} , in particular, the density of the second largest cluster s_2 and the average size of finite

*Electronic address: kownacki@ptm.u-cergy.fr

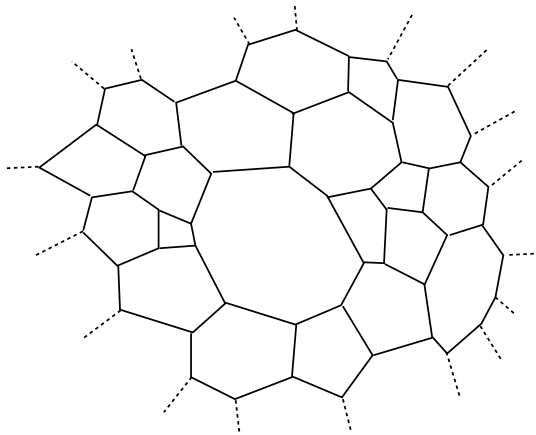


Figure 1: A Φ^3 planar graph

clusters S . Considering k_{max} as a continuous parameter, it is possible to extract a critical parameter k_c similar to a percolation threshold, and to compute critical exponents β , γ and ν associated to the second largest cluster, average cluster size and correlation length. These exponents are compared with those of uniform percolation problem on random Φ^3 planar graphs.

This paper is organized as follows: in section II, we introduce the model of planar Φ^3 random graphs; in section III, targeted attacks are defined and results of numerical simulations are reported; the problem is described as non-uniform percolation and critical exponents are extracted from numerical results in section IV; section V contains conclusions and perspectives.

II. RANDOM Φ^3 PLANAR GRAPHS

We consider the class of trivalent planar graphs, *i.e.* all graphs without boundaries that can be drawn on a sphere and where each vertex is connected to exactly three neighbors. Moreover, two distinct vertices are connected by at most one link and no vertex is connected to itself. An example of Φ^3 graph is shown in figure 1.

For a given number of vertices N , all graphs can be obtained by gluing together N trivalent vertices in all possible ways satisfying the strong constraint of planarity. The Euler characteristic $\chi = N - N_l + N_f$, where N , N_l , and N_f are, respectively, the number of vertices, links and faces, is fixed by the topology so that all planar graphs with the topology of a sphere share the same value $\chi = 2$. One more constraint, arising from the fact that each link is bounded by two vertices and that three links intersect at each vertex, reads $2N_l = 3N$. These constraints imply that N_f and N_l are fixed if N is fixed.

By giving each graph G a Boltzmann weight $w(G)$, this class is turned into a statistical model of random graphs. In this paper, we choose $w(G) = 1$ for each graph. The partition function is given by

$$Z_N = \sum_{G \in \Phi^3|_N} \frac{1}{C(G)}$$

where the sum is over all Φ^3 graphs with N vertices as defined above. $C(G)$ is a symmetry factor which avoids the overcounting of some symmetric graphs and is almost always equal to one for large graphs. There is an apparent regularity in these graphs. Namely connectivity, number of vertices, links and faces are fixed so that these graphs locally look like the honeycomb lattice. Moreover, the average size of a face, *i.e.* the number of links surrounding a face, is equal to six for large N . However, the size of a face is, in fact, a random variable following a distribution $P(Q)$ exactly known [10, 11] (see figure 2), and the correlations associated to the variable Q are long range, decreasing as $1/r^2$ where r is the geodesic distance [9]. Note that for a face (i) with size Q_i , the deviation of Q_i from the average value $\langle Q \rangle = 6$ defines the curvature $R_i \propto (Q_i - 6)/Q_i$.

This implies that these graphs are very different from the honeycomb lattice at large distance. For instance, there are objects called baby universes that induce a self-similar structure for these graphs. A baby universe is a connected part of a graph linked to it by a boundary called a neck. If we call B the size of a baby-universe and l the linear dimension of its neck, we must have $l \ll B^{1/2}$, *i.e.* each baby universe is connected to the rest of the graph by a small boundary. On trivalent graphs, the minimum size of a neck is $l = 3$, and baby universes with such necks are

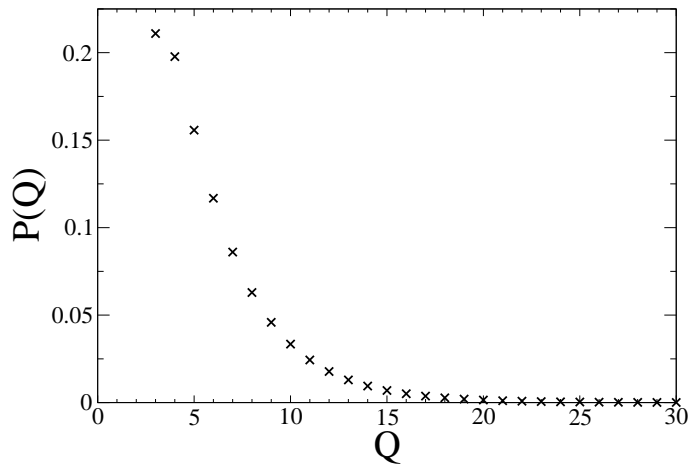


Figure 2: Distribution of the size of the faces

called minimum neck baby universes (minbus). There are more of minbus than of the other baby universes and their distribution has been exactly calculated [12]. Moreover, baby universes can grow on other baby universes, so that each graph is like a tree made of a central part (the root) on which several branches of baby universes are growing. The global spherical topology ensures that branches do not intersect. This tree has a self-similar structure that can be seen as follows: consider the family of baby universes with a given ratio $f = l/\sqrt{B}$ between the linear size l of their neck and the square root of their size B . In a way, f defines a family of baby universes with the same shape. Then, let $a(B \rightarrow 2B, f)$ be the (average) fraction of the total area of a graph included in baby universes with a shape characterized by f and with size ranging from B to $2B$. It can be shown that $a(B \rightarrow 2B, f)$ is independent of B . So, if we probe a graph, it looks similar at any scale, at least in the limit of large graphs.

The fractal structure of these graphs described above is characterized by a Hausdorff (fractal) dimension $d_H = 4$ [13]. This dimension is defined by the scaling law

$$\langle N_r \rangle \sim r^{d_H}$$

where $\langle N_r \rangle$ is the average number of vertices at (geodesic) distance lower than r from any arbitrary vertex.

III. TARGETED ATTACK AND ROBUSTNESS OF PLANAR Φ^3 RANDOM GRAPHS

A. Definitions

A targeted attack is a process that systematically removes highly connected nodes of a graph. In fact, as each vertex of a Φ^3 graph is always trivalent, we define targeted attack as nonrandom removal of faces - instead of vertices - with large number of edges. Note that, as Φ^3 planar graphs are dual to planar triangulations, this is equivalent to nonrandom removal of highly connected vertices of a triangulation.

We introduce a cutoff number k_{max} and define the removal process as follows: for a given graph G , we list all faces whose size - defined as the number of their edges - is greater than k_{max} . Then, each face in this list is removed, *i.e.* all vertices and links which belong to its edges are removed. The resulting amputated graph \tilde{G} is generally not connected. Instead, \tilde{G} consists in a collection of connected smaller planar graphs called connected clusters. As we consider the statistical ensemble $\Phi^3|_N$ of planar Φ^3 random graphs with N vertices, we are interested in average properties under targeted attacks, namely the properties of a graph \tilde{G} associated to a graph G picked at random in $\Phi^3|_N$.

Robustness of a graph to targeted attacks means its ability to preserve its large scale connectivity after a nonrandom deletion of its highly connected nodes. This can be measured by its diameter, defined as the average geodesic distance between two arbitrary nodes, *i.e.* the average length of the shortest path between two arbitrary nodes [2]. Alternatively, as the effect of targeted attacks is to fragment graphs into smaller connected clusters, robustness can be measured by the average density of the largest connected cluster [1], denoted P in this paper. Graphs in $\Phi^3|_N$ are connected, so that P is equal to one before any targeted attack. To get more insight on the consequences of targeted attacks, we also measure the density of the second largest cluster, denoted s_2 , and the mean size of finite clusters,

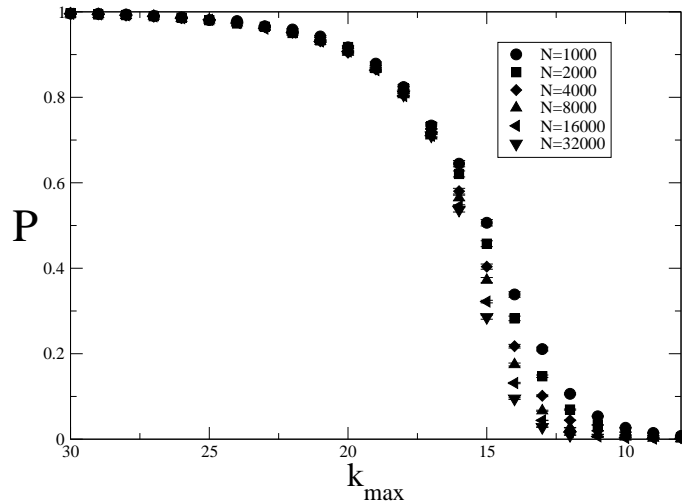


Figure 3: Density of the largest cluster versus k_{max} .

denoted S . The exact definition of S is the following [14]

$$S = \sum'_s s^2 n(s) / \sum'_s s n(s)$$

where $n(s)$ is the average number of clusters made of s vertices and \sum'_s means that the largest cluster is excluded from the sum.

B. Numerical experiment

We generated graphs in $\Phi^3|_N$ following the method described in appendix A. For each graph in a Monte-Carlo series, we performed nonrandom removal of faces - for a given value of k_{max} - and measured the size of the largest connected cluster by a method described in appendix B. We simulated graphs in $\Phi^3|_N$ with N ranging from 1000 to 32000, and the parameter k_{max} ranging from 8 to 30 for each value of N , except for $N = 32000$ where k_{max} was ranging from 12 to 18. For each couple (N, k_{max}) , we made 512 measurements separated by 1000 N_l local updating moves (flips) called T_1 moves (see appendix B). Errors were estimated using the standard jackknife method and error bars are systematically plotted in the figures.

C. Results

The density of the largest cluster P is plotted as a function of the cut-off k_{max} in figure 3. As expected, for very large k_{max} , $P \simeq 1$ as graphs in $\Phi^3|_N$ are connected. We can see that for values of $k_{max} \gtrsim 17$, P slowly decreases with k_{max} , independently of the sizes of the graphs. Then, there is a fast fall of P down to zero. The falling rate is more and more pronounced when the size is increased. This means that a targeted attack with k_{max} greater than about 17 does not significantly affect the connectivity of the graphs - *i.e.*, for these values of k_{max} , more than 70% of the vertices belong to the giant cluster. Conversely, k_{max} has to be smaller than about 13 to completely fragment the graphs into small clusters.

The average fraction of removed vertices is called x_{rm} . It is a smooth decreasing function of k_{max} as can be seen in figure 4. It is interesting to plot P against x_{rm} . This is shown in figure 5.

We can see that a targeted attack significantly affects the connectivity only when a large fraction of the vertices are removed. For example, $P \gtrsim 0.7$ for $x_{rm} \lesssim 0.13$ and $P \gtrsim 0.5$ for $x_{rm} \lesssim 0.17$. In this sense, we can say that planar Φ^3 random graphs are rather robust to targeted attacks.

The analysis of the density of the second largest cluster s_2 and of the average size of finite clusters S , plotted in figures 6 and 7 respectively, gives more information on the mechanism of fragmentation of graphs under targeted attacks. For large k_{max} , $s_2 \simeq 0$, meaning that most of vertices belong to the largest cluster. Then, s_2 sharply increases when k_{max} decreases and eventually reaches a peak for $k_{max} \simeq 15$. This is due to a small gradual decrease of the

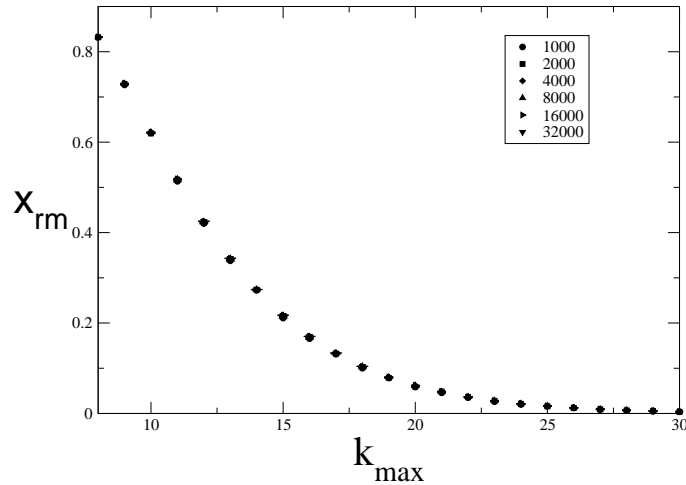
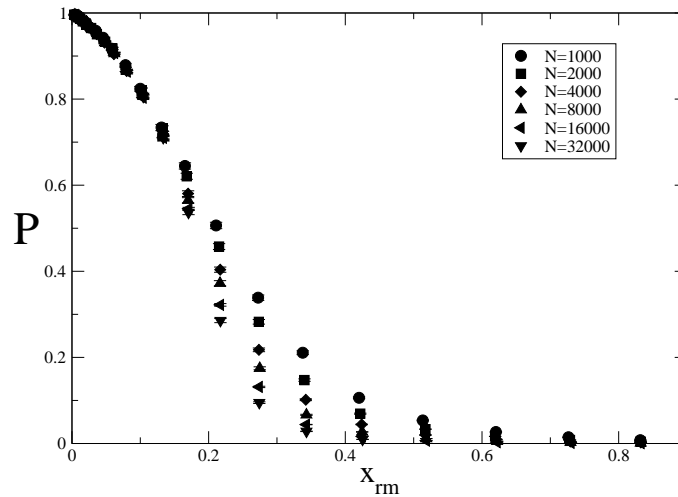
Figure 4: Fraction of removed vertices versus k_{max} 

Figure 5: Density of the largest cluster versus the fraction of removed vertices

connectivity, *i.e.* a small fraction of vertices get disconnected from the largest cluster. However, this phenomenon is marginal as s_2 does not exceed 0.15 and S is not greater than about 8% of the size. So, in this region $k_{max} \gtrsim 15$, the largest cluster completely dominates with only a few number of much smaller clusters. This is corroborated by the behavior of S in this region. As the largest cluster is excluded from this quantity, $S \simeq 0$ for very large k_{max} . As k_{max} decreases, S is essentially influenced by the second, third, etc, largest clusters and so it increases and reaches also a peak. Then, when k_{max} continues to increase, *i.e.* when s_2 and S go through their peak, there is a dramatic change in the fragmentation process. P undergoes a fast drop, meaning that there is an acceleration in the fragmentation and more and more vertices get disconnected from the initial largest cluster. The behaviors of s_2 and S are similar. This is due to the fact that more and more small clusters appear, so that their average size is small, even for the largest, second largest, third largest, etc, clusters.

IV. NON-UNIFORM PERCOLATION

A. Percolation threshold

The fragmentation process described above is very similar to the percolation mechanism [14]. This is, in fact, expected as nonrandom removal of nodes under targeted attack is equivalent to percolation with non-uniform occupation probability [1]. In the case studied here, a vertex is occupied if and only if it does not belong to an edge of a face

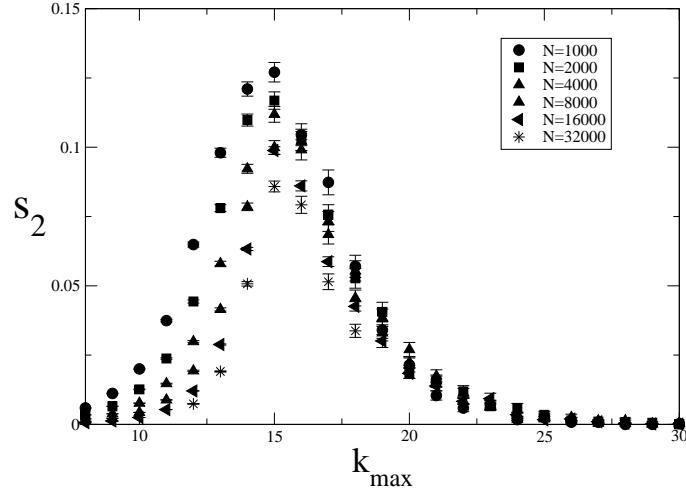


Figure 6: Density of the second largest cluster versus k_{max}

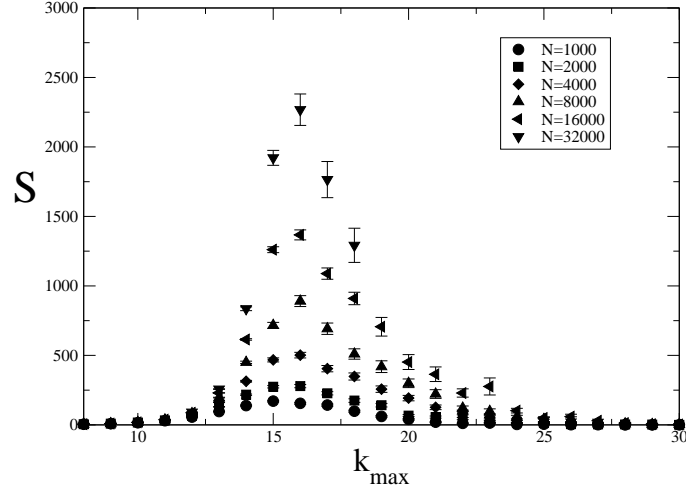


Figure 7: Average size of finite clusters versus k_{max}

whose size is greater than k_{max} . The behavior of P , s_2 and S can then be interpreted by saying that there exists a critical value $k_c \simeq 15$ so that percolation takes place for $k \geq k_c$. In the following, we consider k_{max} as a continuous parameter; more precisely, it is as if the observables P , s_2 and S were defined for all real (positive) values of k_{max} but that numerical data were available only for integer values of k_{max} . Note that k_{max} can be seen as a cutoff on the local scalar curvature. By taking an appropriate continuum limit when $N \rightarrow \infty$, the curvature is, of course, a continuous observable so that a cutoff on curvature has to be continuous in this limit. In other words, in any process of coarse graining, k_{max} would effectively become a continuous parameter.

In order to get a more precise value of k_c , we define a finite size critical parameter $k_c(N)$ as the value of k_{max} for which s_2 is maximum for N fixed. By fitting the data of s_2 with a Gaussian curve, we obtained $k_c(N)$. The result is shown in figure 8. The behavior of $k_c(N)$ can be estimated by standard finite size scaling analysis (see appendix C). This allows us to predict the behavior of $k_c(N)$ approaching k_c as $k_c(N) - k_c \sim N^{-1/\nu d_H}$ with $\nu > 0$ a constant explained in section IV B. So, we fitted the values of $k_c(N)$ with the law $k_c(N) = k_c + c N^{-1/\nu d_H}$, with c a constant. We obtained $k_c = 15.8(2)$.

B. Critical exponents ν , β and γ

The point of view of non-uniform percolation with a percolation threshold k_c strongly suggests that the observables S and s_2 should obey the following scaling laws for k_{max} near k_c [14, 15] (recall that we consider here k_{max} as a

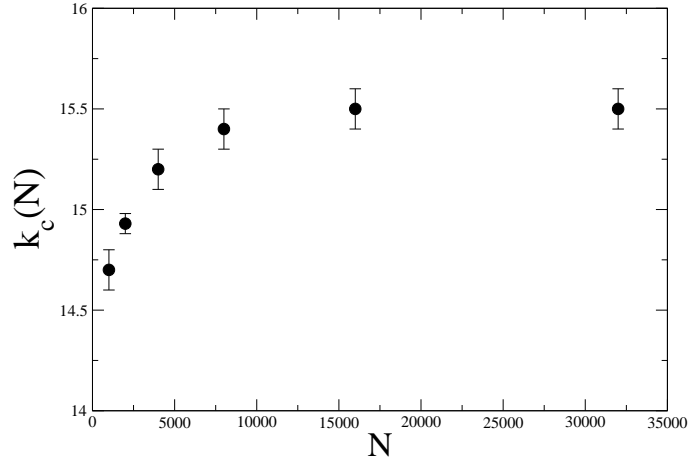


Figure 8: Finite size critical parameter $k_c(N)$

continuous parameter)

$$\begin{aligned} s_2 &\sim (k_{max} - k_c)^\beta \\ S &\sim (k_{max} - k_c)^{-\gamma} \end{aligned}$$

Their finite size counterparts are

$$\begin{aligned} s_2(N) &\sim N^{-\beta/\nu d_H} F \left[(k_{max} - k_c) N^{-1/\nu d_H} \right] \\ S(N) &\sim N^{\gamma/\nu d_H} G \left[(k_{max} - k_c) N^{-1/\nu d_H} \right] \end{aligned}$$

with F and G two scaling functions. The exponent ν characterizes the correlation length associated with a percolation transition. In particular, this exponent controls the way $k_c(N)$ tends to its infinite size value k_c . So, the fit performed in the previous section also allows us to extract the value of ν . The result is $1/\nu d_H = 0.4(2)$. In order to extract the values of exponents β and γ , we have measured the maximum of s_2 and S , which should scale as

$$\begin{aligned} s_2^{max}(N) &\sim N^{-\beta/\nu d_H} \\ S^{max}(N) &\sim N^{\gamma/\nu d_H} \end{aligned}$$

The results are shown in figures 9 and 10. We fitted the data and obtained $\beta/\nu d_H = 0.105(5)$ and $\gamma/\nu d_H = 0.77(1)$.

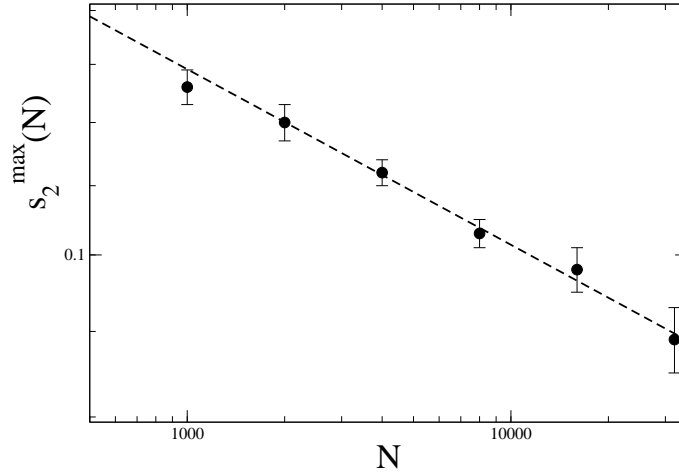


Figure 9: Maximum of density of the second largest cluster versus N , in logscale. The dotted line is the best fit

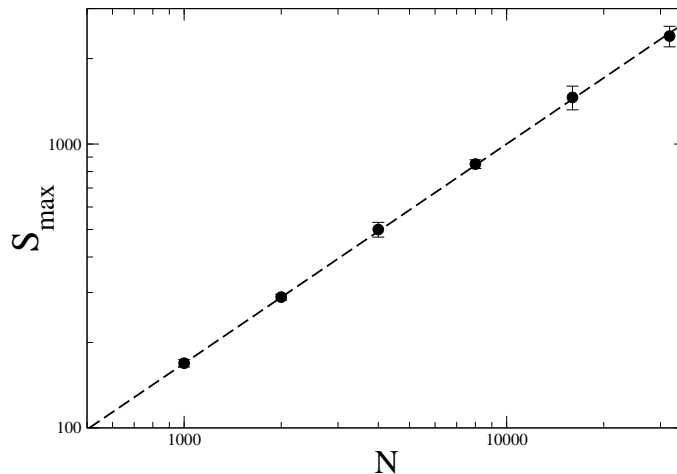


Figure 10: Maximum of the average cluster size versus N . The dotted line is the best fit

C. Systematic errors

Because of the discrete nature of the parameter k_{max} , there are no available data for non-integer values of this parameter. This inevitably induces systematic errors - in particular, values of k_{max} for which observables are maximum - certainly underestimated in the standard analysis used here.

D. Comparing with uniform percolation exponents

Critical exponent are known exactly for uniform percolation on planar Φ^3 random graphs [7], $\beta/\nu d_H = 0.125$, $\gamma/\nu d_H = 0.75$ and $1/\nu d_H = 0.25$. It is tempting to compare them with the values found in this work for non-uniform percolation $\beta/\nu d_H = 0.105(5)$, $\gamma/\nu d_H = 0.77(1)$ and $1/\nu d_H = 0.4(2)$. In view of systematic errors underestimated, it appears that values of exponents β and γ are roughly compatible for uniform and non-uniform percolation. The exponent ν seems very different from the exact value of uniform percolation. However, if we compare it with the value $1/\nu d_H = 0.489(9)$ found in numerical simulations [8], it is once again roughly compatible. In fact, as in uniform percolation, the fractal dimension d_H is very sensitive to finite size effects. However, measures done in this work are not precise enough to conclude that critical exponents are the same for uniform and non-uniform percolation for this problem. It is not excluded either and this would imply a kind of universality between uniform and non-uniform percolation on these graphs.

V. CONCLUSIONS

In the first part of this work, the behavior of planar Φ^3 random graphs under targeted attacks is investigated. The method consists in removing all vertices that belong to an edge of a face whose size is greater than a parameter k_{max} . It appears that this family of graphs is rather robust to this nonrandom removal as k_{max} has to be rather small ($k_{max} \simeq 15$) to significantly affect the global connectivity of these graphs, measured by the density of the largest cluster. This threshold corresponds to the removing of about 20% of the vertices. Note that the case of random failure is equivalent to uniform site percolation. This problem has already been investigated and the high value of the percolation threshold means that these graphs are rather fragile against random failure of nodes.

In a second part, we consider the targeted attacks problem as non-uniform percolation. By measuring two observables characterizing percolation clusters, namely the density of the second largest cluster s_2 and the mean size of connected clusters S , and by extrapolating values of k_{max} to non-integer values, we extract a critical value $k_c = 15.8(2)$ that can be interpreted as a percolation threshold for targeted attacks. It is also possible to look for scaling laws of observables in the vicinity of k_{max} , by analogy to the uniform percolation problem. This allows us to measure (effective) standard critical exponent β , γ and ν . Taking into account underestimated systematic errors due to the fact that k_{max} is, in fact, a discrete parameter, critical exponents found here appear roughly compatible with their counterparts of uniform percolation. This is a very interesting fact as it would show that non-uniform and uniform

percolations are in the same class of universality. If true, this property could be a result of the hierarchical nature of these graphs that makes them look like trees of baby universes (BUs).

Indeed, consider a vertex in a BU. For uniform percolation, a necessary condition for this vertex to belong to a giant cluster is that at least one vertex in the neck of the BU belongs to this giant cluster. The probability for this condition is rather small as necks are very small regions of the graph, so that the probability for a vertex to belong to a giant cluster is smaller if the vertex is in a BU. Consider now the case of targeted attacks. The probability for a vertex to be removed is, in fact, greater if it is in a BU as, on average, there is more curvature in BUs. Then, the probability that a vertex is in the boundary of a large face is greater if the vertex is in a BU. So, in both cases (uniform percolation and targeted attacks), the structure of BUs induces the same effect: the probability to be occupied is smaller for a vertex in a BU. However, this conjecture of universality between uniform and non-uniform percolation has to be more extensively and precisely investigated.

Appendix A: GENERATING AND SAMPLING Φ^3 GRAPHS

The Monte-Carlo sequence starts with a graph in $\Phi^3|_N$ randomly generated as follows: we start from a tetrahedron and, then, add vertices one by one in randomly chosen faces (triangles). Each new vertex is linked to the vertices of the corresponding triangle. The process is repeated until we obtain a graph (polyhedron) with N triangles. This graph becomes a Φ^3 graph - denoted G_o^N - by duality, *i.e.* by replacing each triangle of the polyhedron by a vertex linked to the vertices replacing the adjacent faces of the initial triangle. The resulting graph is topologically equivalent to a sphere with N trivalent vertices. Then, a series of graphs is obtained by using standard flips of links (T_1 moves shown in figure 11) performed on randomly chosen links. It has been shown [10] that T_1 moves define an ergodic transformation in the ensemble $\Phi^3|_N$, so that whatever the starting graph G_o^N , we obtain a nonbiased sampling with this method.

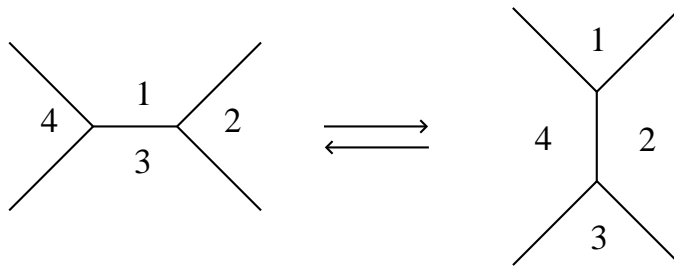


Figure 11: T_1 move involving faces 1,2,3 and 4.

Appendix B: CLUSTER STRUCTURE

In order to measure the connected cluster structure of graphs after a targeted attack, we use a breadth-first search algorithm similar to the Wolff algorithm [16]. It recursively constructs all clusters for a given graph as follows: at "time" n , clusters c_1, c_2, \dots, c_n have already been detected. All sites in these clusters are labeled "visited". At time $n+1$, a not yet visited site (called v_o) is chosen. By definition, it does not belong to any cluster already detected. v_o is the root of the new cluster c_{n+1} ; it is then labeled "visited" and put in a (empty) list Q . The following procedure is now recursively applied to Q : for each site v in Q , all not yet visited neighbors of v (on the graph) are added to c_{n+1} , labeled "visited" and put in Q whereas v is removed from Q . The procedure stops when Q is empty. Then, cluster c_{n+1} is completely constructed. The algorithm stops when all sites have been visited.

Appendix C: FINITE SIZE SCALING

Finite size scaling analysis supposes that finite size corrections to scaling laws near a critical parameter k_c are encoded by scaling functions depending on the ratio between the linear size L of the system and the correlation length ξ . When $L \gg \xi$, finite size effects should not affect the system and scaling laws undergo no correction. On the contrary, when ξ and L become comparable, finite size corrections of scaling laws are expected. For an observable O depending on a parameter k , an infinite size scaling law $O \sim (k - k_c)^{-z}$ can be rewritten $O \sim \xi^{z/\nu}$ as the correlation

length scales as $\xi \sim (k - k_c)^{-\nu}$. In particular, $\xi \sim L$ implies $O \sim L^{z/\nu}$. This can be summarized by the following law: $O \sim L^{z/\nu} F((k - k_c) L^{1/\nu})$ with $F(x)$ a (scaling) function of the dimensionless ratio $x = (k - k_c) L^{1/\nu} \sim (L/\xi)^{1/\nu}$. In order to interpolate between the cases $L \gg \xi$ and $L \sim \xi$, $F(x)$ must verify $F(x) \rightarrow 1$ for $x \sim 1$ and $F(x) \rightarrow x^{-z}$ for $x \gg 1$. Finite size scaling is a powerful tool for extracting critical exponents by studying the variations of observables with the size of the system. This also provides a natural finite size critical parameter $k_c(L)$: suppose that $F(x)$ reaches a maximum for $x = x_o$. Then, for fixed L , the value of k giving a maximum for O obeys the following relation $(k - k_c) L^{1/\nu} = x_o$ or, equivalently, $k_c(L)$ approaches k_c when the size becomes infinite as $k_c(L) - k_c \sim L^{-1/\nu}$ [14]. However, graphs in $\Phi^3|_N$ have no explicit linear size, but the quantity N^{1/d_H} , where d_H is the Hausdorff dimension, plays this role so that finite size scaling laws are $O \sim N^{z/\nu d_H} F((k - k_c) N^{1/\nu d_H})$ and $k_c(N)$ approaches k_c as $k_c(N) - k_c \sim N^{-1/\nu d_H}$.

-
- [1] D. S. Callaway, M.E.J. Newman, S. H. Strogatz and D. J. Watts, 2000 *Phys. Rev. Lett.* **85** 5468
 - [2] R. Albert, H. Jeong and A.-L. Barabasi, 2000 *Nature (London)* **406** 378
 - [3] A. Broder, R. Kumar, F. Maghoul, P. Raghavan, S. Rajagopalan, R. Sata, A. Tomkins and J. Wiener, 2000 *Comput. Netw.* **33** 309
 - [4] R. Albert and A.-L. Barabasi, 2002 *Rev. Mod. Phys.* **74** 47 ; S.N. Dorogovtsev, A.V. Goltsev and J.F.F. Mendes, *arXiv:0705.0010*.
 - [5] D.S. Callaway, M.E.J. Newman, S. H. Strogatz and D. J. Watts, *Phys. Rev. Lett.* , 2000 **85** 5468 ; R. Cohen, D. ben-Avraham and S. Havlin, 2002 *Phys. Rev. E* **66** 036113 ; Z. Wu, C. Lagorio, L.A. Braunstein, R. Cohen, S. Havlin and H.E. Stanley, 2007 *Phys. Rev. E* **75** 066110; J.D. Noh, 2007 *Phys. Rev. E* **76** 026116; H.D. Rozenfeld and D. ben-Avraham, 2007 *Phys. Rev. E* **75**, 061102
 - [6] F. David, *Gravitation and Quantizations*, 1992 *Les Houches Session LVII* (Elsevier, Amsterdam); J. Ambjørn, *Fluctuating Geometries and Field Theory*, 1994 *Les Houches Session LXII* (Elsevier, Amsterdam); P. Di Francesco, P. Ginsparg and J. Zinn-Justin, 1995 *Phys. Rep.* **254** 1; J. Ambjørn, B. Durhuus, and T. Jonsson, *Quantum Geometry*, 1997 (Cambridge University Press, Cambridge).
 - [7] V.A. Kazakov, 1988 *Nucl. Phys. B (Proc. Supp.)* **4** 93; V.A. Kazakov, 1989 *Mod. Phys. Lett. A* **4** 1691 (1989)
 - [8] J.-P. Kownacki, 2008 *Phys. Rev. Phys. Rev. E* **77** 021121
 - [9] W. Janke, D.A. Johnston and M. Weigel, 2006 *Condens. Matter Phys.* **9** 263; W. Janke and M. Weigel, 2004 *Phys. Rev. B* **69** 144208
 - [10] D.V. Boulatov, V.A. Kazakov, I.K. Kostov and A.A. Migdal, 1986 *Nucl. Phys. B* **275** 641
 - [11] C. Godrèche, I. Kostov and I. Yekutieli, 1992 *Phys. Rev. Lett.* **69** 2674
 - [12] S. Jain and S.D. Mathur, 1992 *Phys. Lett. B* **286** 239
 - [13] H. Kawai, N. Kawamoto, T. Mogami and Y. Watabiki, 1993 *Phys. Lett. B* **306** 19; J. Ambjørn and Y. Watabiki, 1995 *Nucl. Phys. B* **445** 129
 - [14] D. Stauffer and A. Aharony, 1994 *Introduction to Percolation Theory* (Taylor & Francis, New York)
 - [15] A. Margolina, H.J. Herrmann and D. Stauffer, 1982 *Phys. Lett. A* **93** 73
 - [16] U. Wolff, 1989 *Phys. Rev. Lett.* **62** 361